Check for updates

Received: 18 December 2020 | Revised: 18 February 2021 | Accepted: 19 February 2021

DOI: 10.1002/jmr.2893

RESEARCH ARTICLE

Journal of Molecular Recognition WILEY

Chemical binding of pyrrolidinyl peptide nucleic acid (acpcPNA-T9) probe with AuNPs toward label-free monitoring of miRNA-21: A novel biosensing platform for biomedical analysis and POC diagnostics

Nazanin Fathi[1,2] | Arezoo Saadati[3] | Mohammad Hasanzadeh[1] | Mohammad Samiei[4]

[1]Pharmaceutical Analysis Research Center, Tabriz University of Medical Sciences, Tabriz, Iran

[2]Research Center for Immunodeficiencies, Pediatrics Center of Excellence, Children's Medical Center, Tehran University of Medical Sciences, Tehran, Iran

[3]Food and Drug Safety Research Center, Tabriz University of Medical Sciences, Tabriz, Iran

[4]Faculty of Dentistry, Tabriz University of Medical Sciences, Tabriz, Iran

Correspondence
Mohammad Hasanzadeh, Pharmaceutical Analysis Research Center, Tabriz University of Medical Sciences, Tabriz, Iran.
Email: hasanzadehm@tbzmed.ac.ir

Mohammad Samiei, Faculty of Dentistry, Tabriz University of Medical Sciences, Tabriz, Iran.
Email: samiei.moh@gmail.com

Funding information
Tabriz University of Medical Sciences, Grant/Award Number: 61674-IR.TBZMED.VCR.REC.1397.365

Abstract

miRNAs are attractive factors in cancer research studies due to their important roles for regulating of gene expression. Because of miRNA-21 expression surplus in many types of cancers, so accurate identification is important. Increasing efforts have caused different methods to improve the sensitivity and specificity of detection. Present study is an attempt to report a new electrochemical label-free PNA-based bioassay for detection of miRNA-21. In this study, gold electrode was modified by gold nanoparticles to improve a functional PNA-based biosensor. The EDS and field emission scanning electron microscope (FE-SEM) were used to detect fabrication of biosensor. The electrochemical behavior of sensor was evaluated after inserting of acpcPNA probes and miRNA-21 on the stucture of electrode and analyzed essential parameters such as various concentration of target miRNA, hybridization time, reproducibility, stability, and applicability. The results of study demonstrated that engineered biosensor was successfully fabricated. The findings showed the highest amount of current in 5 minutes hybridization time, with suitable reproducibility and stability. This innovative miRNA-based biosensor presents a sensitive and specific method in fast and may be lab-on chip assay in future.

KEYWORDS
cancer diagnosis, chemical binding, gold nanoparticle, miRNA-21, peptide nucleic acid

1 | INTRODUCTION

MicroRNAs or miRNAs are small noncoding RNAs about 18 to 27 nucleotides and are presently receiving considerable attention due to extensive role in various cellular processes like modulation of gene expression and development of cancer.[1,2] Some of these miRNAs like miRNA-21 have shown over-expression pattern in many types of cancers. So, great efforts have been made to the design of the better analysis methods for detecting of theses valuable biomarkers.[3,4] Despite, technology development applied to find more sensitive and selective methods in miRNA detection such as nanoparticle-based amplification,[5] isothermal exponential amplification,[6] hybridization chain reaction (HCR),[7] and rolling circle amplification (RCA).[8] But microarray analysis, northern blotting and quantitative polymerase chain reaction (qPCR) as traditional methods are still widely used. So, developing more practicable and efficient methods remains as a challenge.

Nowadays, biosensors are developing rapidly as an innovative research area in analytical biology by providing advantages such as simple, rapid, sensitive, and low-cost detection and promising approach to point-of-care diagnostics.[9-11] Electrochemical and optical biosensors

Nazanin Fathi and Arezoo Saadati are co first author.

 © 2021 John Wiley & Sons Ltd.

as well as other emerging technologies developed for highly sensitive miRNA detection. Among these methods, electrochemical miRNA biosensors because of superior advantages including simplicity of miniaturization, high sensitivity and selectivity, good detection limits with small analyte volumes, functional diversity, and relatively low cost have made them a suitable option for nucleic acids analysis.[12,13]

This technique typically was designed based on the change in electrochemical signal which generates via the hybridization of the probe, a supplementary single-stranded nucleotide, and the target miRNA,[14] that it is suitable for low-concentration agents like miRNAs which are usually present only in femto- or nanomolar quantities in plasma.[15] Selection of the appropriate probe is one of the most important steps in electrochemical miRNA biosensors design.

Peptide nucleic acid (PNA) is synthesized in polymer homologs of DNA which in variable deoxyribose phosphate backbone are altered to pseudo-peptide that appraised as a higher specificity probe for miRNA detection.[16] It presents unique advantages such as stability against chemicals, proteases, and nucleases compared with natural oligonucleotides, hence enhances the efficiency of hybridization.[17] Pyrrolidinyl PNA with D-prolyl-2-aminocyclopentanecarboxylic backbone (acpcPNA) exists unique properties for binding to RNA such as qualified biological stability and a highly sequence-specific manner with superior mismatch discrimination capacities than other DNA probes. These advantages of acpcPNA provide a promising platform for genosensors.[18]

In present study, in addition to applying label-free method due to further simplifying and even properly cost-effective, we applied gold nanoparticles (AuNPs) as a common modifier of electrode surface. AuNPs are well known to unique electronic and catalytic properties, with a great potential effective immobilization, widely use in electrochemical miRNA biosensor.[19-23]

This study's aim was reporting a new electrochemical label-free miRNA biosensor, by AuNPs-modified gold electrode (Au). The monitoring of current change was performed by recording of CVs in the presence of standard EC probe (Ferro-Ferri) which reducing of oxidation peak currents happened due to increases in the surface insulation and block the electrons transfer. The construction stages of the developed genosensor were analyzed by different pivotal parameters such as hybridization time and concentration of miRNA. The performances of the designed biosensor were evaluated by stability, reproducibility, as well as applicability of it in plasma.

2 | MATERIALS AND METHODS

2.1 | Chemical and reagents

Sodium acetate (CH_3COONa), hydrogen tetrachloroaurate (III) hydrate ($HAuCl_4{\cdot}3H_2O$), citric acid, potassium chloride (KCl99.8% purity), sodium hydroxide (NaOH), potassium ferrocyanide ($K_4Fe(CN)_6$), potassium ferrocyanide ($K_3Fe(CN)_6$), TB (toluidine blue), DTT (dithiotrietol), MCE (mercaptoethanol), 11-mercapto-1-undecanol (11-MUL), and polyvinyl pyrrolidone (PVP) K-30 were attained from Sigma-Aldrich (Ontario, Canada). Diethyl pyrocarbonate (DEPC) treated water was consumed to prepare the miRNA stock solution. Buffer solutions were used as follows: 10 mM tris(hydroxymethyl)aminomethane-HCl (tris-HCl, pH 7.80) for miRNA21 dilution and immobilization, H_2SO_4 for electrode washing, and HEPES (*N*-2-hydroxyethylpiperazine-*N*-ethanesulfonic acid) buffer solution. All sample tubes, microtips, and glassware were treated with DEPC to minimize the effect of RNases on the stability of miRNAs and autoclaved to inactivate traces of DEPC. The oligonucleotide sequences achieved from Takapouzist Co. (Iran) include: The 9-mer C-terminal lysine-modified acpcPNA (Ac-TTTTTTTTT-LysNH_2) denoted "acpcPNA-T9 probe," were synthesized according to the published protocol. All the target oligonucleotides used in this study were synthesized and purified through BioRP by Bioneer Co., Korea. The complementary DNA and miRNA were preliminarily used to study the electrode's fabrication and optimization parameters.

The acpcPNA-T9 probe': TTTTTTTTTLysNH_2.

miRNA-21:5′-rUAGCUUAUCAGACUGAUGUUGA-3′.

Dilution of oligonucleotides was performed using Tris-HCl buffer (0.1 M, pH ~ 7.4). Electrochemical studies were carried out using supporting electrolyte containing 0.5 mM $K_4Fe(CN)_6/K_3Fe(CN)_6$ (1:1) and 0.5 mM of KCl.

2.2 | Equipment

The Ag/AgCl (saturated KCl) and platinum wire were applied as reference and auxiliary electrode, respectively. Also, the gold electrode (GE) with 2 mm diameter (from Azar Electrode Co., Urmia, Iran) was applied as working electrode. An unexceptional three-electrode system's (from Metrohm, Autolab B.V., The Netherlands) electrochemical measurements were done using a PalmSense 4c system (Palm instruments, Utrecht, The Netherlands) that controlled by PSTrace 5.3 software. Field emission scanning electron microscope (FE-SEM) (Tescan Mira3, Czech) was performed to appraise the modified electrode surface and particles morphology. The chemical composition of the modified electrodes was investigated using energy dispersive spectroscopy (EDS). Square wave voltammetry (SWV) evaluations were performed using E_{pulse} = 0.005 V, pulse amplitude = 0.001 V, and frequency = 10.0 Hz. The electrode modification process was investigated by electrochemical impedance spectroscopy (EIS) over a frequency range of 10 kHz to 1 mHz with an AC voltage amplitude of 0.010 V vs Ag/AgCl with a Pt wire counter-electrode using a Autolab Type III electrochemical impedance analyzer (Methrom Autolab B.V., The Netherlands). The impedance spectra were fitted to a Randle's equivalent circuit by the FRA software to obtain the charge transfer resistance (R_{ct}).

2.3 | Construction of the electrochemical PNA-based biosensor

For cleaning, GE was burnished by using 0.05 μm alumina slurry (Beuhler, USA), and then a three-electrode system was placed inside a cell containing 0.5 M H_2SO_4, and 25 repetitive cycles were carried up in the potential range from −0.2 to 2 V and scan rate of 100 mV s^{-1}. After that, GNPs were provided by adding HEPES solution, prepared using 0.5 M H_2SO_4, to 20 mM of $HAuCl_4$.

To fabricate the PNA-based biosensor, HEPES-prepared GNPs were electrodeposited on the superficies of the GE by chronoamperometry (ChA) technique with 500 seconds duration time at E = 0.0 V (Figure 1). Then, acpcPNA-T9 (probe) was immobilized on the superficies of the modified electrode and was incubated for 12 hours at 4°C. Next, the nonreact space of modified electrode with the probe was blocked by using mercaptoethanol (MCE). Moreover, MCE leads to boost DNA take-up in the next step (11). After incubation at room temperature for 30 minutes, designed PNA-based biosensor was utilized for hybridization of DNA-A9. The electrochemical PNA-based biosensor design steps were exhibited in Scheme 1.

3 | RESULTS AND DISCUSSION

3.1 | The FE-SEM and EDS characterization

To evaluate modification of GNPs on gold electrode as well as immobilization of probe and hybridization of miRNA-21, FE-SEM images were recorded which are illustrated in Figure 2. As shown in this figure, as in forward steps, GNPs/GE; acpcPNA-T9/GNPs/GE; and miRNA21/acpcPNA-T9/GNPs/GE changing in electrode was obviously apparent. Therefore, the electrode was successfully modified with GNPs, acpcPNA-T9 probe, and target miRNA; consequently, desirable PNA-based biosensor was stabilized by conforming this morphology of electrode. The small-sized GNPs with spherical structure arranged on the electrode surface demonstrated that the GNPs were assembled onto it. Incubating of the acpcPNA-T9 probe on GNPs/GE also created some changes in the electrode morphology which is characterized in high magnification. Therefore, acpcPNA-T9 probe was successfully immobilized on the GNPs/GE. Moreover, incubating of target miRNA-21 on acpcPNA-T9/GNPs/GE revealed obviously clear changes in morphology of the electrode, as showed in Figure 2. These illustrations could confirmed successful arrangement of proposed PNA-based biosensor.

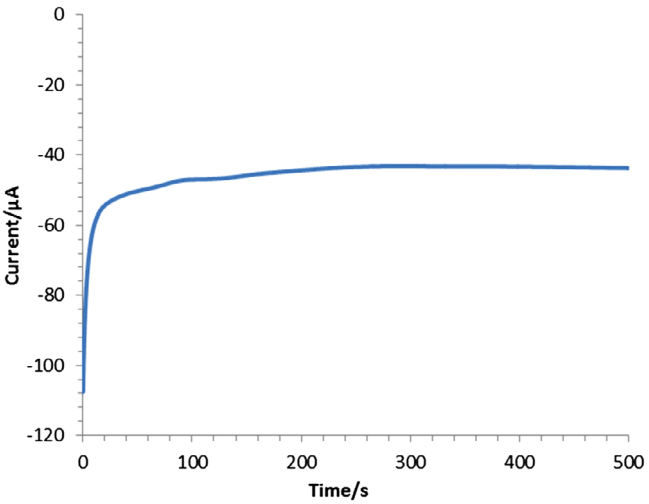

FIGURE 1 Chronoamperogram of gold electrode in the presence of 0.5 M H_2SO_4, to 20 mM of $HAuCl_4$ (duration time = 500 s, E = 0.0 V)

Furthermore, determination of modified electrodes and miRNA-21/acpcPNA-T9 hybridization is also performed using a chemical composition analysis by energy dispersive spectroscopy (EDS). As showed in Figure 3, electrochemical-deposited GNPs on gold electrode determined Au elements' presence in higher concentration on the electrode. These results confirm the successful modification of the electrode. Adding acpcPNA-T9 revealed new elements like O, N, and P that are basic elements in organic structures, as well as in acpcPNA-T9, that is a pyrrolidinyl PNA with D-prolyl-2-aminocyclopentanecarboxylic acid (ACPC) backbone. Mentioned results indicated that assembling the acpcPNA-T9/GNPs/GE structures was successfully established. Eventually, inserting of miRNA to previous mentioned step revealed a different sharp and very large peaks related to O and N elements which represent miRNA was hybridized with acpcPNA-T9 probe. These results confirmed a successful assembling of designed miRNA-21 biosensor.

3.2 | Electrochemical compartment

The electrochemical behavior of electrode surface preparation was followed by EIS techniques using the classic ferrocyanide/ferricyanide redox couple as reporter with conducting in the potential range of −0.22 to 0.005 V and in a frequency range of 0.1 Hz to 100 kHz. The results obtained from EIS in the base of charge transfer resistance

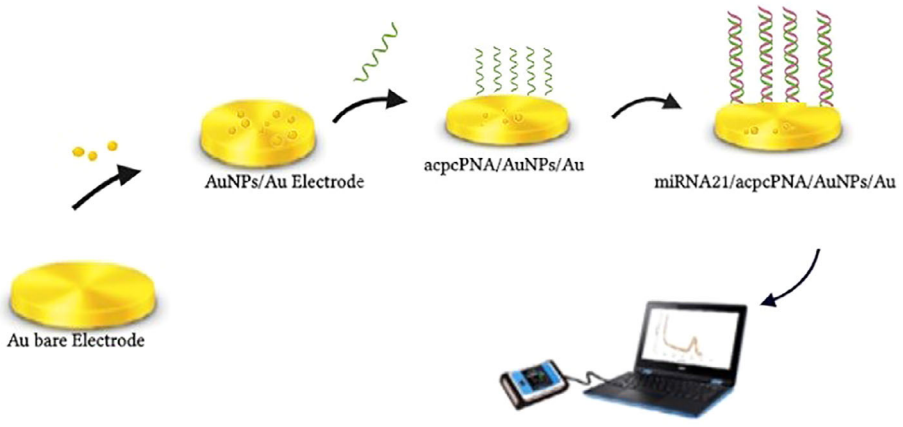

SCHEME 1 The schematic presentation of the fabrication process of PNA-based biosensor

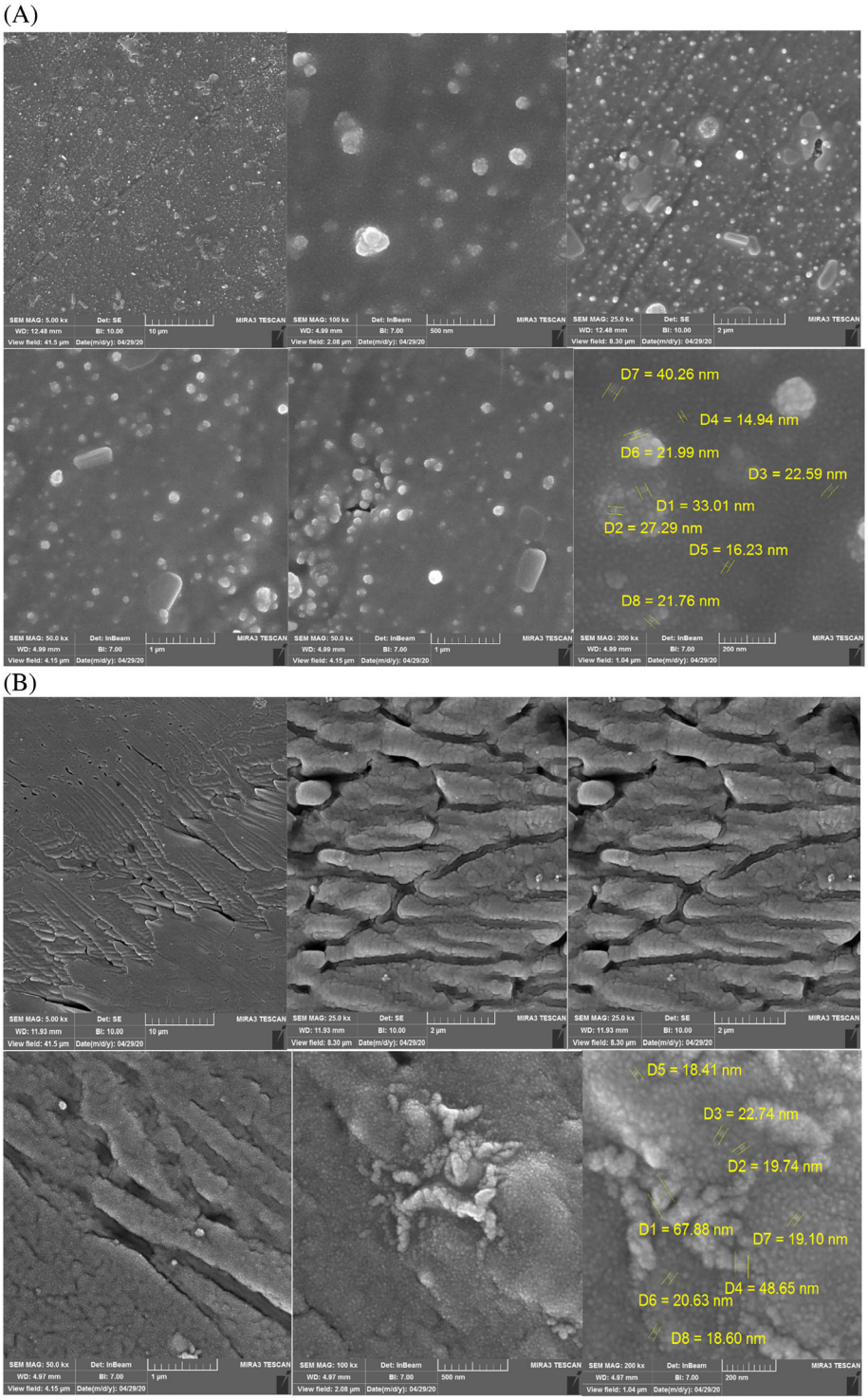

FIGURE 2 FE-SEM images of GNPs/GE, A, acpcPNA-T9/GNPs/GE, B, and miRNA21/acpcPNA-T9/GNPs/GE, C. These images demonstrate the changes in the surface of Au electrode after acpcPNA-T9 step

(R_{ct}) in the high-frequency region showed a semicircle diameter. This form of values was attained by fitting the data as appropriate equivalent circuit. As shown in Figure 4, the bare Au electrode shows virtually a linear part that demonstrates the low R_{ct} that demonstrated an insignificant charge transfer resistance. When AuNPs electrodeposited on electrode surface, the higher amount of R_{ct} (Ω) has been revealed. These results were conformed the suitable preparation of expected modification on the Au electrode was achieved.

According to stepwise, after electrodeposition of AuNPs on, the C-terminal lysine-modified acpcPNA (Ac-TTTTTTTTTLysNH$_2$) probe was added and incubated 12 hours at 4°C. It was demonstrated that the amine compounds more strongly adsorb on the Au surface and amine-Au bond

(C)

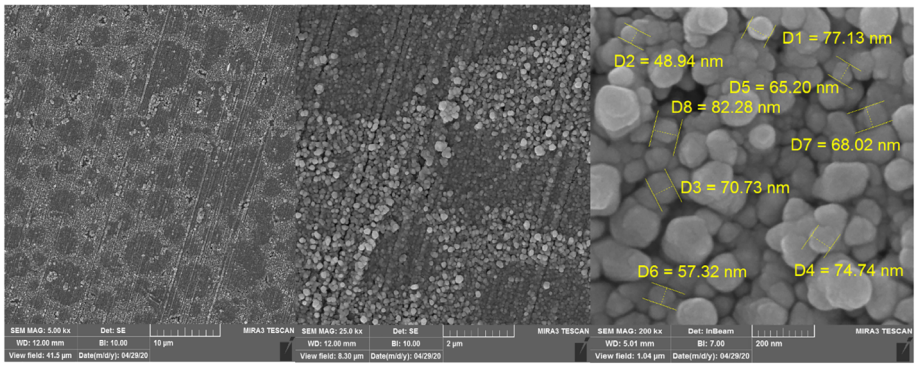

FIGURE 2 (Continued)

being through the nitrogen lone-pair. According to studies, amine compounds significantly established a binding only in an under-coordinated Au atom site. As well as, the energy of adsorption in higher coordinated sites is too low, suggested that molecules can establish stable adsorption in this position. In other words, the amine molecules are practically bound to gold surface and not to other sites that causes amine-modified probe to become a favorable option for using to Au electrodes.[24,25]

When the acpcPNA-T9 is inserted to system (acpcPNA-T9/GNPs/GE), a much slightly increased the R_{ct}.

In the next step, after incubation time of previous prepared electrodes were washed with bi-distilled water to eliminate the unabsorbed probes, then was added 5 μL of 1 mM MCE and incubated in room temperature for 30 minutes. MCE adsorbs strongly on gold surface to block the exposed Au electrode and prevents more adsorption of other components.[26] The R_{ct} increased further with added MCE (MCE/acpcPNA-T9/GNPs/GE) because it was blocked the more charge transfer by uncovered GNPs. Subsequently, for determining the successfully fabrication of biosensor, a DNA-A9 which has a complementary sequence with the acpcPNA-T9 probe was tested (DNA-A9/MCE/acpcPNA-T9/GNPs/GE). The EIS results showed that the hybridization of DNA-A9 to probe on the electrode surface (DNA A9/MCE/acpcPNA-T9/GNPs/GE) creates a significant increase of the R_{ct} due to more blocking of the charge. The serial changes of R_{ct} confirmed that designed biosensor was effectively manufactured. Finally, determination of appropriate miRNA hybridization with acpcPNA-T9 probe is typically depending on the electrochemical behavior changes in presence and absence of target miRNA.

3.3 | Optimization of miRNA hybridization time

Optimum hybridization time between probe and its complementary target miRNA is a key factor for determining appropriate function of prepared sensor. For this purpose, after immobilization of 5 μL of miRNA-21 on the prepared electrode (miRNA-21/MCE/acpcPNA-T9/GNPs/GE) and incubating in 5, 10, 15, 20, and 30 minutes at 37°C. Electrochemical tests were performed in $[Fe(CN)_6]^{3-/4-}$ solution) for defining the optimum hybridization time. Hybridization time tests were typically determined by the changes on the peak current of and resistance in different times. As shown in Figure 5, different incubation time of hybridization of miRNA-21 appears various electrochemical behavior. The finding results by EIS illustrated that the optimal time for incubation of miRNA-21 is 5 minutes. According to Figure 5, the highest amount of current was found in 5 minutes, so this time defined as the optimum time for incubation of miRNA-21.

3.4 | Effect of scan rate

Due to the importance of scan rate as a significant parameter in the examination of the various platforms electrical activity, its effect was evaluated using GNPs modified GE in $[Fe(CN)_6]^{3-/4-}$ solution by CV technique with scan rate range from 2 to 1000 mV s^{-1} (Figure 6A). As can be seen in Figure 6B, scan rate in the range of 30 to 500 mV s^{-1} has a linear relationship with peak current, that it indicates the control of mass-transfer through the diffusion process. In addition, the dependence of ln I_{pa} vs ln v and I_p vs $v^{0.5}$ is utilized as two significant factors to assess whether the reaction is controlled by the adsorption or diffusion process, as well as its reversibility. These curves are revealed in Figure 6 for oxidation peak. In the absence of kinetic complications at reversible or irreversible systems, I_p and $v^{0.5}$ are associated and cross the origin of the plot. As can be seen in Figure 6, I_{pa} and $v^{0.5}$ curve is linear (R^2 = .9985) and crosses the axes of origin, which is expounded by the following equation:

$$I_{pa}\,(\mu A) = 239.72\,v\,(V/s)^{0.5} - 3.9821\,(R_2 = .9985)$$

This dependence crosses the origin, which indicates that the reaction is controlled by diffusion. In the selected range of sweep rate (2-1000 mV s^{-1}), the dependence of ln I_{pa} vs ln v is also linear and expounded by the following equation:

$$\mathrm{Ln}\,I_{pa}\,(\mu A) = 0.5219\,\mathrm{Ln}\,v\,(V/s) + 5.4664\,(R_2 = .9984)$$

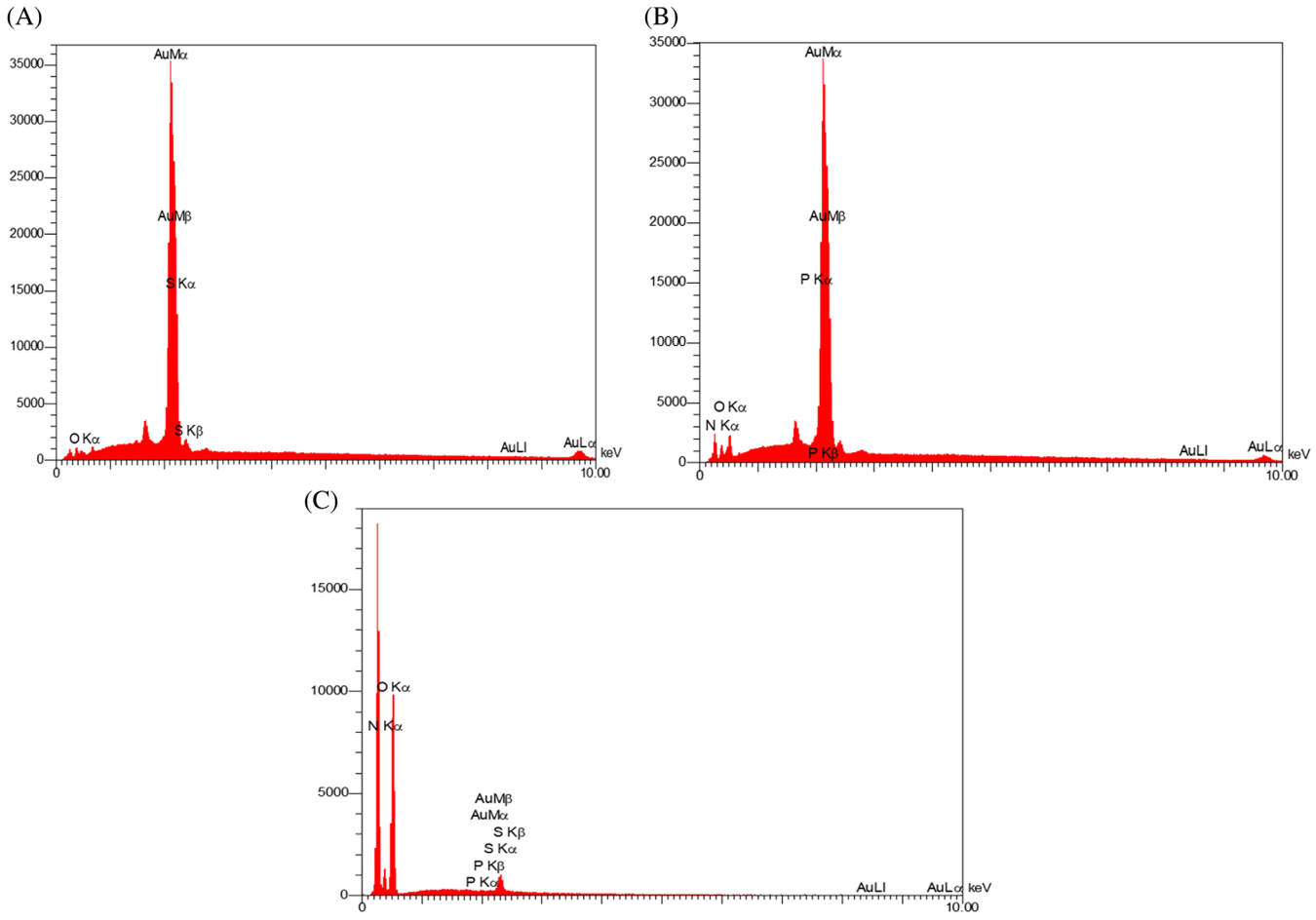

FIGURE 3 EDS spectra of, A, GNPs/GE, B, acpcPNA-T9/GNPs/GE, C, miRNA-21/acpcPNA-T9/GNPs/GE

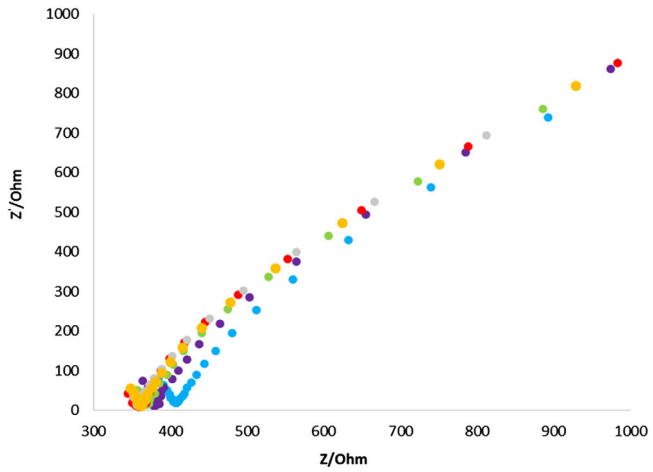

FIGURE 4 Nyquist plots of the impedance spectra from 0.1 Hz to 100 kHz for various steps of modification of gold electrode (GNPs/GE, acpcPNA-T9/GNPs/GE, MCE/acpcPNA-T9/GNPs/GE, DNA-A9/MCE/acpcPNA-T9/GNPs/GE and miRNA-21/MCE/acpcPNA-T9/GNPs/GE). Supporting electrolyte = $[Fe(CN)_6]^{3-/4-}$/KCl). E pulse = 0.005 V, pulse amplitude = 0.001 V, and frequency = 10.0 Hz

Its slope is 0.5219 and indicates diffusion-control of the reaction. A slope close to 1 and 0.5 is associated to reaction control with adsorption and diffusion, respectively.[27]

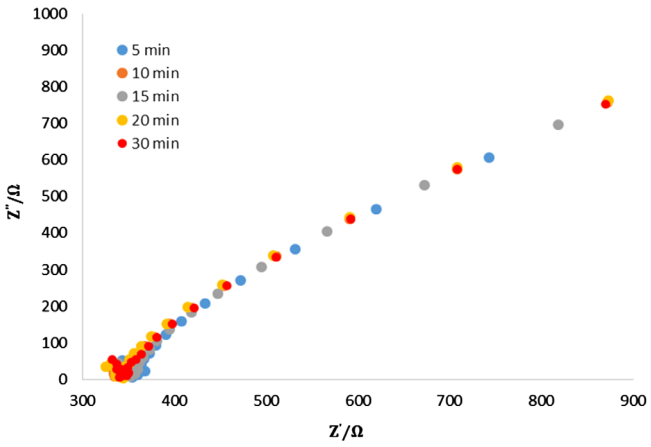

FIGURE 5 Nyquist plots of the impedance spectra from 0.1 Hz to 100 kHz for the biosensor after target miRNA incubation in various times (5-10-15-20-30 min). Supporting electrolyte = $[Fe(CN)_6]^{3-/4-}$/KCl). E pulse = 0.005 V, pulse amplitude = 0.001 V, and frequency = 10.0 Hz

The dependence of E_{pa} on sweep rate is revealed in Figure 6E. Since in irreversible electrochemical reactions, the E_{pa} and sweep rate are independent of each other; it can be concluded that the electron transfer in this reaction is irreversible, because as a result of increasing the sweep rate, E_{pa} also increases.[28,29]

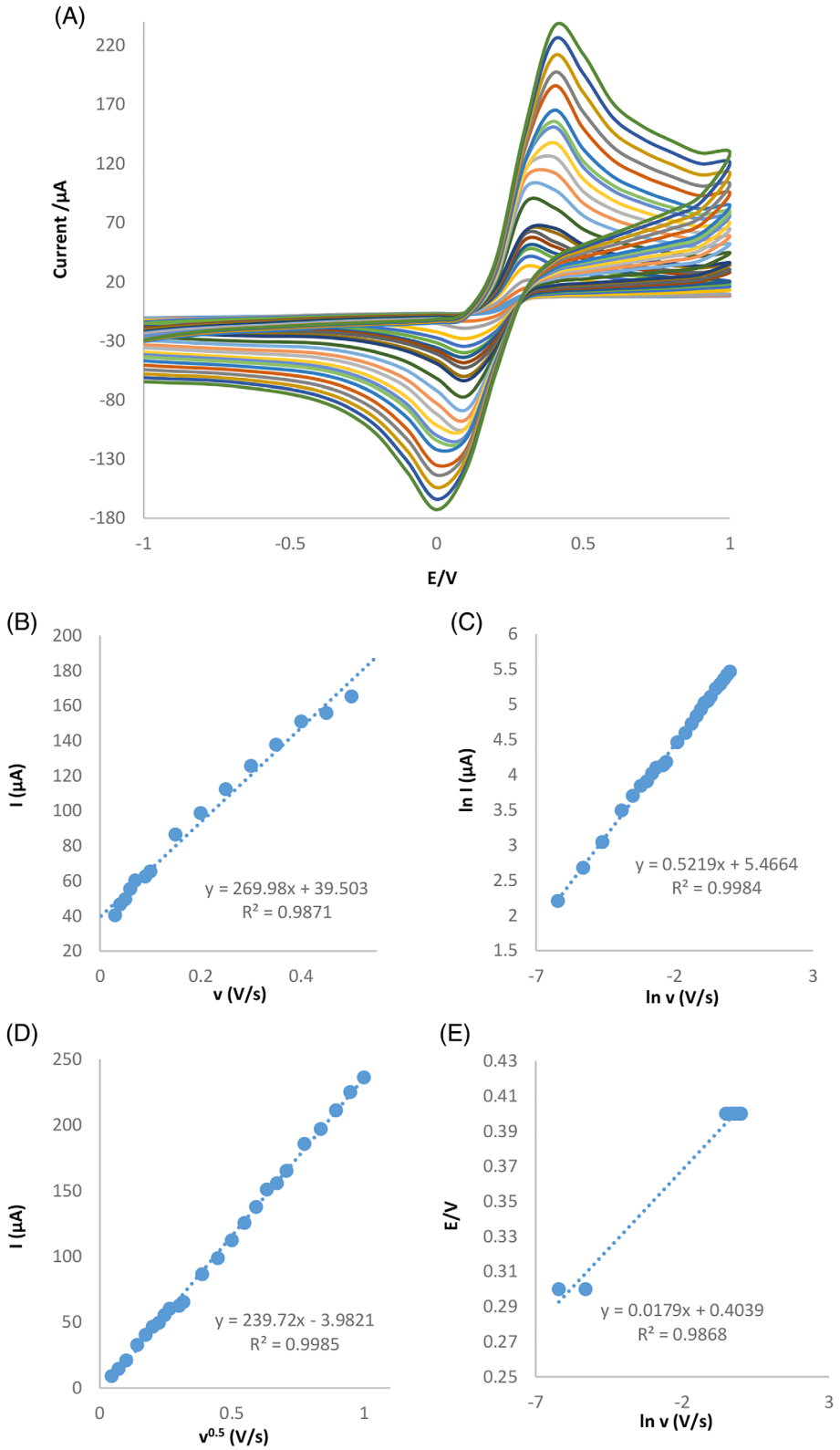

FIGURE 6 A, CVs of GNPs/GE in the $[Fe(CN)_6]^{3-/4-}$ solution in diverse sweep rates (2, 5, 10, 20, 30, 40, 50, 60, 70, 90, 100, 150, 200, 250, 300, 350, 400, 450, 500, 600, 700, 800, 900, 1000 mVs^{-1}); B, dependency of oxidation peak currents vs sweep rate; C, the plot of Neperian logarithm of oxidation peak current vs Neperian logarithm of sweep rates; D, dependency of oxidation peak currents vs square root of sweep rates; E, dependency of anodic peak potential vs Neperian logarithm of sweep rates

3.5 | Analytical performance

The execution of PNA-based biosensor was assessed by hybridization of acpcPNA-T9 with various concentrations of miRNA-21 (10^{-6}, 10^{-8}, 10^{-10}, 10^{-12}, 10^{-14}, 10^{-16}, 10^{-18}, 10^{-20}, and 10^{-22} M) after incubation at 37°C for 20 minutes (Figure 7). The achieved results manifest an increase in the peak current resulting from an increment in target concentration. The calibration plot was delineated under optimum conditions between logarithm of oxidation peak current and logarithm of miRNA-21 concentration. Linear range and lower limit of quantification (LLOQ) were acquired using DPV technique from 1×10^{-6} M to 1×10^{-22} M and 1×10^{-22} M, respectively. The plot phase bode of biosensor at different

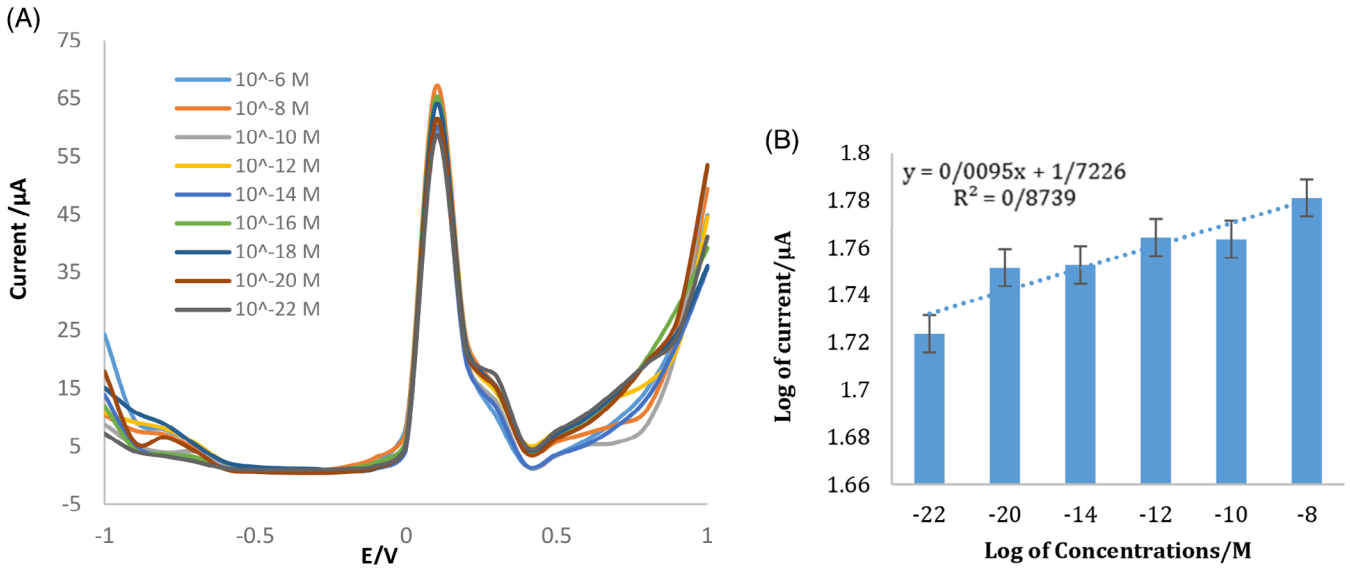

FIGURE 7 A, DPVs of the engineered PNA-based biosensor in different concentrations of miRNA-21 (10^{-6}, 10^{-8}, 10^{-10}, 10^{-12}, 10^{-14}, 10^{-16}, 10^{-18}, 10^{-20}, and 10^{-22} M), B, calibration plots (supporting electrolyte = $[Fe(CN)_6]^{3-/4-}$/KCl). E pulse = 0.005 V, pulse amplitude = 0.001 V, and frequency = 10.0 Hz

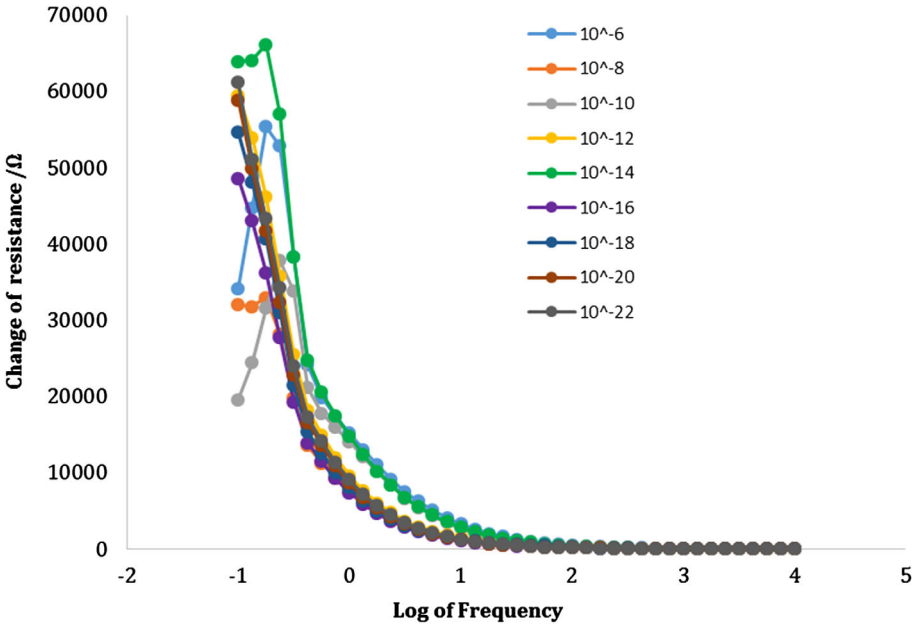

FIGURE 8 The plot of oxidation peak current vs logarithm of frequency. Supporting electrolyte = $[Fe(CN)_6]^{3-/4-}$/KCl. Frequency = 0.1 Hz to 100 kHz

target concentrations of analyte is presented in Figure 8. The results reveal the high capability of engineered PNA-based biosensor for detection of miRNA-21. In comparison to other methods,[29-32] this biosensor is more sensitive. So, this sensor is able to being a potential technique for recognizing low amounts of miRNA-21 (Table 1).

3.6 | Assessment of the PNA-based biosensor specificity (selectivity study)

In this study for determination, the rate of specific recognition of miRNA-21 by designed biosensor was utilized from the single base and double bases mismatched miRNAs. The results achieved from CV and EIS techniques are showed in Figure 9. These results illustrated that the miRNA-21 has more increase in peak current than another two complementary RNAs that derived from almost high affinity to hybridization with acpcPNA-T9 probe on the modified electrode surface. Noticeably, more reduction in peak of current was determined in double mismatch than single once. One or two bases could not alter the rate of current in designed system. This is owing to inconsistent bases and deficient hybridization with probe sequences on the superficies. The results reveal that the designed PNA-based biosensor has high capability for selective and discrete detection of target miRNA-21.

TABLE 1 Comparison between the diverse methods sensitivity to identification of miRNA-21

Method	Substance	Linear area	LOD/LLOQ	Reference
The smartphone-based biosensor	rGO/Au electrode	1×10^{-4} M to 1×10^{-12} M	1×10^{-4}	Li et al[29]
The electrochemical biosensor	CHA and rolling RCA	0.5 to 12 500 pmol	290 fmol	Lu et al[30]
The electrochemical biosensor	TSP and DSN	0.1 fM to 0.1 pM	0.04 fM	Zouari et al[31]
Amperometric biosensor	HRP	0.096 to 25 pM	29 fM	Chen et al[32]
The electrochemical PNA-based biosensor	GNPs/GE	1×10^{-6} M to 1×10^{-22} M	0.1 zM	This work

Abbreviations: CHA, catalytic hairpin assembly; DSN, duplex-specific nuclease; HRP, horseradish peroxidase; RCA, rolling circle amplification; rGO/Au, reduced graphene oxide/gold; TSP, tetrahedron-structured probes.

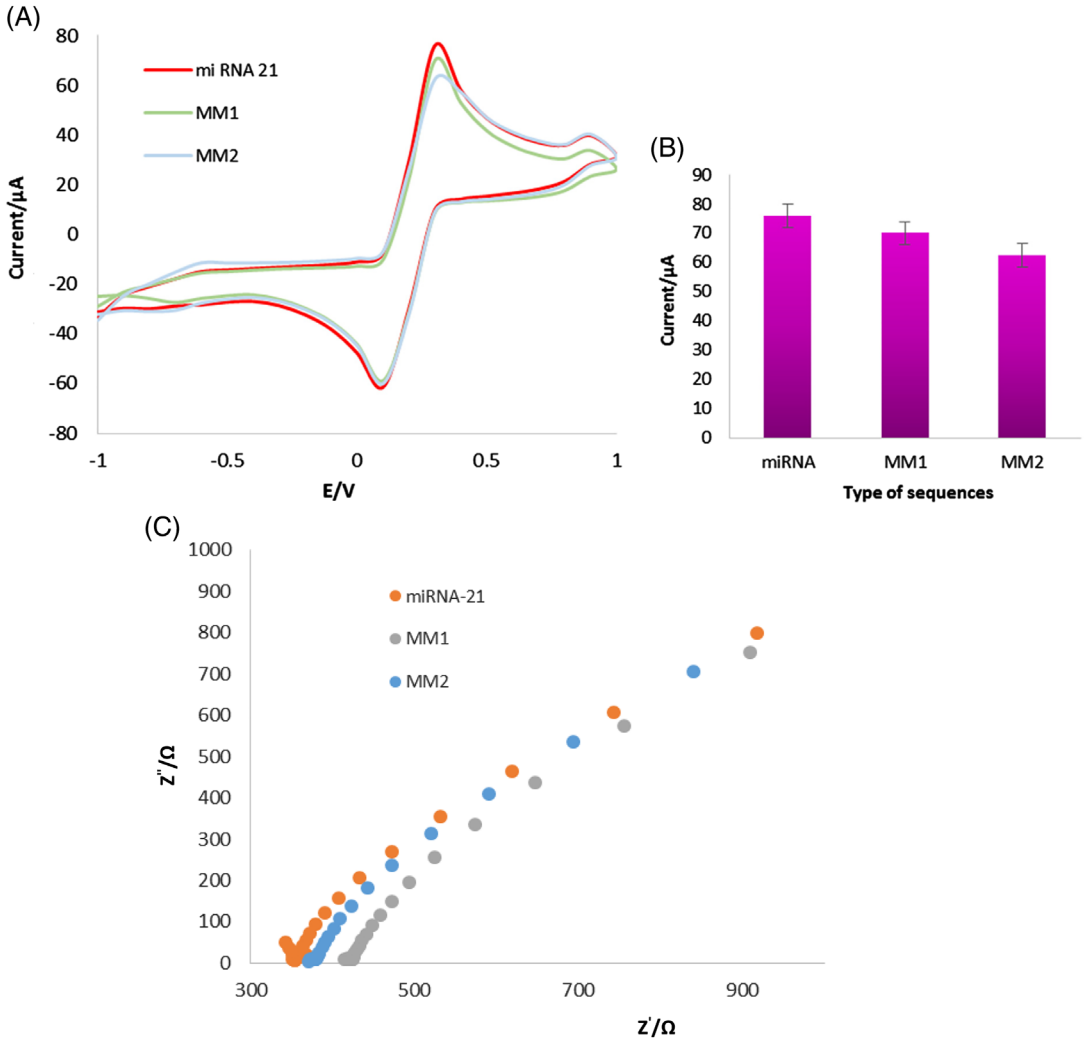

FIGURE 9 A, CVs, of PNA-based biosensor for hybridization by target miRNA-21, single base and double bases mismatched miRNAs. (Supporting electrolyte = $[Fe(CN)_6]^{3-/4-}$/KCl). B, Histogram of peak currents vs type of sequences. C, Nyquist plots of the impedance spectra of PNA-based biosensor for hybridization by target miRNA-21, single base and double bases mismatched miRNAs. (Supporting electrolyte = $[Fe(CN)_6]^{3-/4-}$/KCl). Frequency = 0.1 Hz to 100 kHz

3.7 | Assessment of the PNA-based reproducibility and stability

Reproducibility is an essential factor defining the applicability of developed biosensor. It was calculated by the relative standard deviation (RSD) via this equation:

$$\%\text{RSD} = \text{Standard deviation (SD)} / \text{average of detection values (Mean)}$$

The RSD results obtained from measuring of repeating construction process of modified electrodes (acpcPNA/AuNPs/GE) were showed that the %RSD of average measurements was calculated to be 7.75% (Figure 10). Therefore, these results indicated the

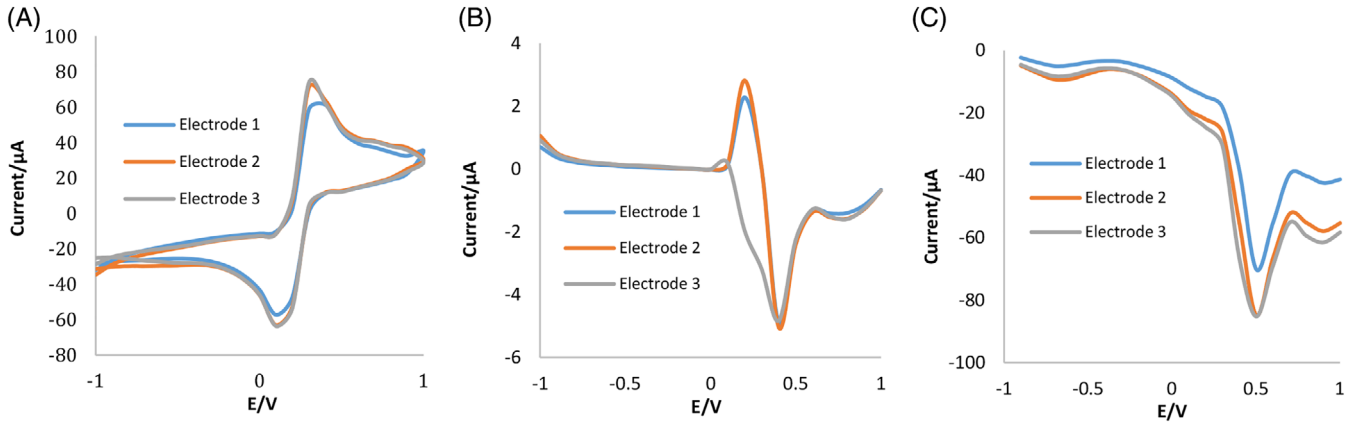

FIGURE 10 Interelectrode stability of GNPs/GE. A, CVs, B, DPVs, C, SWVs (supporting electrolyte = $[Fe(CN)_6]^{3-/4-}$/KCl). (Supporting electrolyte concentration 0.5 mM). E_{pulse} = 0.005 V, pulse amplitude = 0.001 V, and frequency = 10.0 Hz

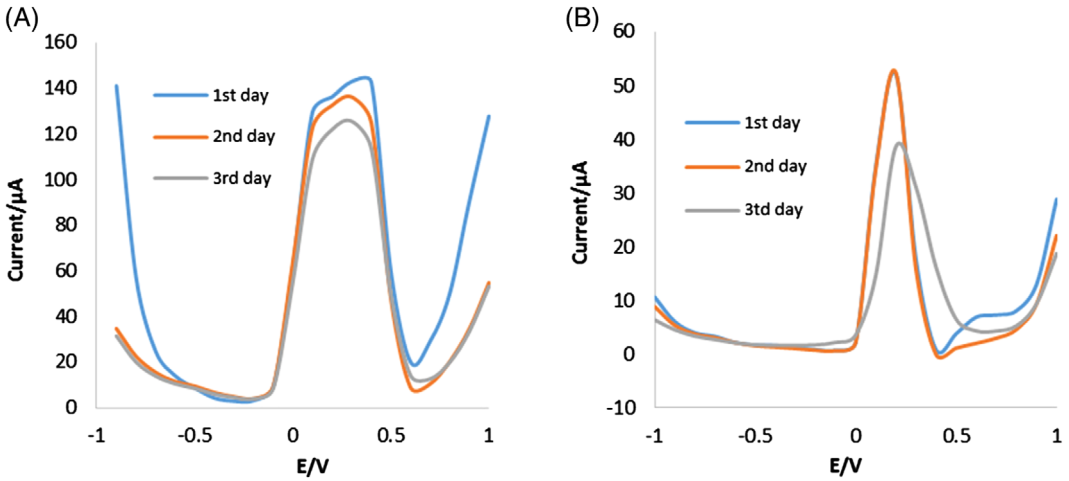

FIGURE 11 Intraday stability of acpcPNA-T9/GNPs/GE. A, CVs, B, DPVs (supporting electrolyte = $[Fe(CN)_6]^{3-/4-}$/KCl) in different time of storage (1-3 days). (Supporting electrolyte concentration 0.5 mM). E_{pulse} = 0.005 V, pulse amplitude = 0.001 V, and frequency = 10.0 Hz

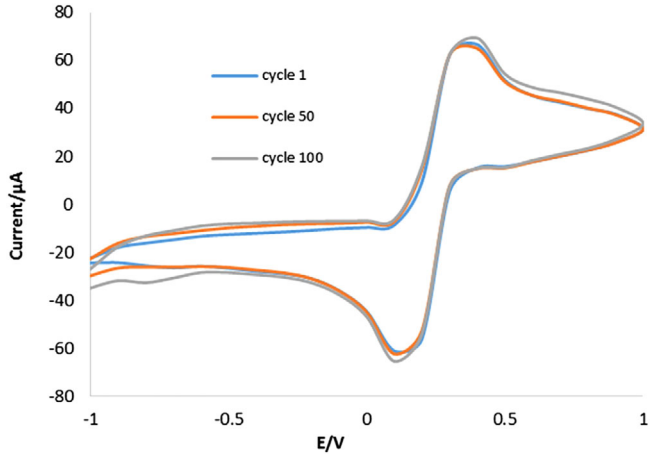

FIGURE 12 Cyclic stability of GNPs/GE (supporting electrolyte = $[Fe(CN)_6]^{3-/4-}$/KCl). (Supporting electrolyte concentration 0.5 mM). E_{pulse} = 0.005 V, pulse amplitude = 0.001 V, and frequency = 10.0 Hz

designed genosensor has acceptable reproducibility. According to the Clinical and Laboratory Standards Institute (CLSI), RSD <10% for stability and reproducibility are required.[26]

Stability presents the change of detection signals in a period that a biosensor be storage. Hence, calculating the stability of biosensors to optimizing the best storage time for determining of its performance is important. For this purpose, we measured the CV, DPV, and SWV of acpcPNA-T9/GNPs/GE independently under same conditions between 3 days by preserving them at 4°C in the dark condition. The results presented in Figure 11 indicate a decrease in the performance of the proposed sensor day by day. Therefore, it can be concluded that the best performance of this sensor is provided on the same day, and after 2 days, it loses its efficiency. Furthermore, the cyclic stability of the GNPs-modified gold electrode was evaluated by after 1, 50, and 100 cycles. As shown in Figure 12, there are no significant changes in peak of current between tested cycles consequently, the stability of electrode performance was confirmed.

3.8 | PNA-based biosensor response in human plasma samples

A recovery test was conducted to test validation of PNA-based biosensor. For this purpose, different final concentrations of miRNA-21 from 10^{-6} to 10^{-22} M into human plasma samples. Consequently, prepared samples were analyzed by the designed sensor. According to the obtained results, the peak current in high concentrations of miRNA-21 was more than less concentrations in human plasma. The peak of current was gradually reduced in concentrations dependent of miRNA-21 in plasma. The higher rate of hybridization between acpcPNA-T9 and miRNA-21 caused more current compared to when more acpcPNAs was free without hybridization to target miRNA-21. In addition to, achieved results showed a good correlation with a slope of 0.08 and R^2 = .9783. These findings provided evidence that this biosensor may good candidate for detecting of miRNA-21 in biological samples. The lower limit of quantification (LLOQ) of developed sensor was 1×10^{-18} M and linear range was from 1×10^{-18} to 1×10^{-6} M.

4 | CONCLUSION

In present study, an electrochemical PNA-based biosensor was successfully developed by gold nanoparticles (GNPs) modification and pyrrolidinyl peptide nucleic acid (acpcPNA-T9) probe, following the electrochemical behavior after inserting the miRNA-21 as a cancer-related biomarker. AuNPs were used as the current amplification and provide the suitable surface for inserting of probe. Hybridization of miRNA-21 to complement sequence of probe in short time resulted to change the current; therefore, this assay could be applied to fast and sensitive directly detection of miRNA-21 in biological samples with any extra methods. With these advantages, prepared biosensor could be a hopeful method for detection of miRNA in different samples.

ACKNOWLEDGEMENT

This work was supported by TBZMED (Tabriz University of Medical Sciences)-Grant Number 61674-IR.TBZMED.VCR.REC.1397.365.

DATA AVAILABILITY STATEMENT

The data that support the findings of this study are available from the corresponding author upon reasonable request.

ORCID

Mohammad Hasanzadeh https://orcid.org/0000-0003-4918-1239

REFERENCES

1. Naeli P, Yousefi F, Ghasemi Y, Savardashtaki A, Mirzaei H. *The role of microRNAs in Lung Cancer: Implications for diagnosis and therapy*. Curr Mol Med. 2020;20:90-101.
2. Müller S, Janke F, Dietz S, Sültmann H. *Circulating MicroRNAs as Potential Biomarkers for Lung Cancer*. Tumor Liquid Biopsies: Springer; 2020:299-318.
3. Fakhri N, Abarghoei S, Dadmehr M, Hosseini M, Sabahi H, Ganjali MR. *Paper based colorimetric detection of miRNA-21 using Ag/Pt nanoclusters*. Spectrochim Acta A Mol Biomol Spectrosc. 2020;227:117529.
4. Nasirian V, Shamsipur M, Molaabasi F, Mansouri K, Sarparast M, Salim V. *miRNA-21 rapid diagnosis by one-pot synthesis of highly luminescent red emissive silver nanoclusters/DNA*. Sens Actuators B. 2020;308:127673.
5. Dai W, Dong H, Guo K, Zhang X. *Near-infrared triggered strand displacement amplification for MicroRNA quantitative detection in single living cells*. Chem Sci. 2018;9(7):1753-1759.
6. Jia H, Bu Y, Zou B, Wang J, Kumar S, Pitman JL. *Signal amplification of microRNAs with modified strand displacement-based cycling probe technology*. Analyst. 2016;141(22):6297-6302.
7. Zhuang P, Zhang H, Welchko RM, Thompson RC, Xu S, Turner DL. *Combined microRNA and mRNA detection in mammalian retinas by* in situ *hybridization chain reaction*. Sci Rep. 2020;10(1):1-10.
8. Yang J, Tang M, Diao W, Cheng W, Zhang Y, Yan Y. *Electrochemical strategy for ultrasensitive detection of microRNA based on MNAzyme-mediated rolling circle amplification on a gold electrode*. Microchimica Acta. 2016;183(11):3061-3067.
9. Ye J, Xu M, Tian X, Cai S, Zeng S. *Research advances in the detection of miRNA*. J Pharmaceut Anal. 2019;9(4):217-226.
10. Senel M, Dervisevic M, Esser L, Dervisevic E, Dyson J, Easton CD. *Enhanced electrochemical sensing performance by in situ electrocopolymerization of pyrrole and thiophene-grafted chitosan*. Int J Biol Macromol. 2020;143:582-593.
11. Saadati A, Hassanpour S, Hasanzadeh M, Shadjou N. *Binding of pDNA with cDNA using hybridization strategy towards monitoring of Haemophilus influenza genome in human plasma samples*. Int J Biol Macromol. 2020;150:218-227.
12. Kilic T, Erdem A, Ozsoz M, Carrara S. *microRNA biosensors: opportunities and challenges among conventional and commercially available techniques*. Biosens Bioelectron. 2018;99:525-546.
13. Saadati A, Hassanpour S, de la Guardia M, Mosafer J, Hashemzaei M, Mokhtarzadeh A. *Recent advances on application of peptide nucleic acids as a bioreceptor in biosensors development*. TrAC Trends Anal Chem. 2019;114:56-68.
14. Zhao L-L, Pan H-Y, Zhang X-X, Zhou Y-L. *Ultrasensitive detection of microRNA based on a homogeneous label-free electrochemical platform using G-triplex/methylene blue as a signal generator*. Anal Chim Acta. 2020;1116:62-69.
15. Tsujiura M, Ichikawa D, Komatsu S, Shiozaki A, Takeshita H, Kosuga T. *Circulating microRNAs in plasma of patients with gastric cancers*. Br J Cancer. 2010;102(7):1174-1179.
16. Gan W, Xiaoxin SX. *Peptide nucleic acid (PNA) binding-mediated gene regulation*. Cell Res. 2004;14(2):111-116.
17. Liu L, Lu H, Shi R, Peng X-X, Xiang Q, Wang B. *Synergy of peptide-nucleic acid and spherical nucleic acid enabled quantitative and specific detection of tumor exosomal MicroRNA*. Anal Chem. 2019;91(20):13198-13205.
18. Vilaivan T. *Pyrrolidinyl PNA with α/β-dipeptide backbone: from development to applications*. Acc Chem Res. 2015;48(6):1645-1656.
19. Chanho P, Jimin K, Inchul B, Juneseok Y, Kuewhan J, Sungsoo N. *Highly sensitive and selective detection of single-nucleotide polymorphisms using gold nanoparticle MutS enzymes and a micro cantilever resonator*. Talanta. 2019;205:120154.
20. Xiuli F, Yunqing W, Yongming L, et al. *A graphene oxide/gold nanoparticle-based amplification method for SERS immunoassay of cardiac troponin I*. Analyst. 2019;144(5):1582-1589.
21. Zhiyang Z, Zhaopeng C, Fangbin C, Yaowen Z, Lingxin C. *Highly sensitive on-site detection of glucose in human urine with naked eye based on enzymatic-like reaction mediated etching of gold nanorods*. Biosens Bioelectron. 2017;89(Pt 2):932-936.
22. Shasha W, Zhaopeng C, Jaebum C, Lingxin C. *Naked-eye sensitive ELISA-like assay based on gold-enhanced peroxidase-like immunogold activity*. Anal Bioanal Chem. 2016;408(4):1015-1022.

23. Xingyi M, Phuoc LT, Nguyen HA, Sang JS. *Single gold nanoplasmonic sensor for clinical cancer diagnosis based on specific interaction between nucleic acids and protein*. Biosens Bioelectron. 2015;67:59-65.
24. Venkataraman L, Klare JE, Tam IW, Nuckolls C, Hybertsen MS, Steigerwald ML. *Single-molecule circuits with well-defined molecular conductance*. Nano Lett. 2006;6(3):458-462.
25. Hoft RC, Ford MJ, McDonagh AM, Cortie MB. *Adsorption of amine compounds on the Au (111) surface: a density functional study*. J Phys Chem C. 2007;111(37):13886-13891.
26. Banica F-G. *Chemical Sensors and Biosensors: Fundamentals and Applications*. Germany: John Wiley & Sons; 2012.
27. Kissinger P, Heineman WR. *Laboratory Techniques in Electroanalytical Chemistry, Revised and Expanded*. England: CRC Press; 2018.
28. Low SS, Pan Y, Ji D, Li Y, Lu Y, He Y. *Smartphone-based portable electrochemical biosensing system for detection of circulating microRNA-21 in saliva as a proof-of-concept*. Sens Actuators B. 2020;308:127718.
29. Li Q, Zeng F, Lyu N, Liang J. *Highly sensitive and specific electrochemical biosensor for microRNA-21 detection by coupling catalytic hairpin assembly with rolling circle amplification*. Analyst. 2018;143(10):2304-2309.
30. Lu J, Wang J, Hu X, Gyimah E, Yakubu S, Wang K. *Electrochemical biosensor based on tetrahedral DNA nanostructures and G-quadruplex–hemin conformation for the ultrasensitive detection of MicroRNA-21 in serum*. Anal Chem. 2019;91(11):7353-7359.
31. Zouari M, Campuzano S, Pingarrón JM, Raouafi N. *Amperometric biosensing of miRNA-21 in serum and cancer cells at nanostructured platforms using anti-DNA-RNA hybrid antibodies*. ACS Omega. 2018;3(8):8923-8931.
32. Chen L-C, Wang E, Tai C-S, Chiu Y-C, Li C-W, Lin Y-R. *Improving the reproducibility, accuracy, and stability of an electrochemical biosensor platform for point-of-care use*. Biosens Bioelectron. 2020;155:112111.

How to cite this article: Fathi N, Saadati A, Hasanzadeh M, Samiei M. Chemical binding of pyrrolidinyl peptide nucleic acid (acpcPNA-T9) probe with AuNPs toward label-free monitoring of miRNA-21: A novel biosensing platform for biomedical analysis and POC diagnostics. *J Mol Recognit*. 2021;e2893. https://doi.org/10.1002/jmr.2893